·临床研究·

MRI联合^{18}F-FDG PET和^{11}C-MET PET对颅内肿胀性脱髓鞘病变与胶质瘤的鉴别诊断作用

杨亦寒 蔡莉 马海文 王颖 白宇 明浩朗 于圣平 任炳成 林雨 张凯 海龙 王伟 程铖 李涛 杨学军

【摘要】 **目的** 探讨MRI联合^{18}F-脱氧葡萄糖(^{18}F-FDG)PET和^{11}C-蛋氨酸(^{11}C-MET)PET显像对颅内肿胀性脱髓鞘病变与胶质瘤的鉴别诊断价值。**方法** 纳入经病理学直接证实或内科保守治疗间接证实的14例颅内肿胀性脱髓鞘病变患者和17例胶质瘤患者,采用MRI观察病变与周围正常脑组织界限,T_1WI、T_2WI和扩散加权成像(DWI)信号强度,强化征象(包括环状强化和开环状强化等),占位效应,周围脑水肿,病变中心静脉扩张,胼胝体受累,病变中心坏死,灰质受累情况;^{18}F-FDG PET和^{11}C-MET PET显像对代谢程度进行视觉分析。**结果** MRI显示,颅内肿胀性脱髓鞘病变患者占位效应0级8例(8/14)、Ⅰ级4例(4/14)、Ⅱ级1例(1/14)、Ⅲ级1例(1/14),周围脑水肿Ⅰ度12例(12/14)、Ⅱ度2例(2/14);胶质瘤患者占位效应0级2例(2/17)、Ⅰ级6例(6/17)、Ⅱ级7例(7/17)、Ⅲ级2例(2/17),周围脑水肿Ⅰ度7例(7/17)、Ⅱ度10例(10/17),组间差异均有统计学意义(Fisher确切概率法:P = 0.032,0.024)。^{18}F-FDG PET和^{11}C-MET PET显像对颅内肿胀性脱髓鞘病变与胶质瘤的鉴别诊断差异无统计学意义(Fisher确切概率法:P = 0.182,0.081)。**结论** MRI显示的占位效应和周围脑水肿可以用于鉴别诊断颅内肿胀性脱髓鞘疾病与胶质瘤,PET-CT对症状类似胶质瘤的颅内肿胀性脱髓鞘病变无明确诊断价值。

【关键词】 脱髓鞘疾病; 中枢神经系统; 神经胶质瘤; 磁共振成像; 体层摄影术,发射型计算机

MRI combined with ^{18}F-FDG PET and ^{11}C-MET PET in differentiating tumefactive demyelinating lesion and glioma

YANG Yi-han[1], CAI Li[2], MA Hai-wen[1], WANG Ying[2], BAI Yu[1], MING Hao-lang[1], YU Sheng-ping[1], REN Bing-cheng[1], LIN Yu[1], ZHANG Kai[1], HAI Long[1], WANG Wei[1], CHENG Cheng[1], LI Tao[1], YANG Xue-jun[1]

[1]Department of Neurosurgery, [2]PET-CT Center, Tianjin Medical University General Hospital, Tianjin 300052, China

Corresponding author: YANG Xue-jun (Email: ydenny@yahoo.com)

【**Abstract**】 **Objective** To explore the value of MRI combined with ^{18}F-fluoro-2-deoxy-D-glucose (^{18}F-FDG) PET and ^{11}C-methionine (^{11}C-MET) PET on differentiating tumefactive demyelinating lesion (TDL) and glioma. **Methods** Fourteen cases of TDL and 17 cases of glioma were confirmed by pathology directly or internal medicine treatment. MRI was used to observe the lesion boundary, T_1WI, T_2WI and diffusion-weighted imaging (DWI) signal intensity, enhancement (including ring enhancement and open-ring enhancement, etc.), mass effect, peripheral edema, and the presence of central venectasia, corpus callosum engagement, central necrosis and gray matter engagement. ^{18}F-FDG PET and ^{11}C-MET PET were used to calculate relative uptake values. **Results** Among all TDL cases, MRI showed that mass effect of 8 cases (8/14) were grade 0, 4 cases (4/14) grade Ⅰ, one case (1/14) was grade Ⅱ and one case (1/14) grade Ⅲ; the peripheral edema of 12 cases (12/14) were grade Ⅰ and 2 cases (2/14) grade Ⅱ. Among all glioma cases, the mass effect of 2 cases (2/17) were grade 0, 6 cases (6/17) grade Ⅰ, 7 cases (7/17) grade Ⅱ and 2 cases (2/17)

doi:10.3969/j.issn.1672-6731.2017.10.009

基金项目:中国抗癌协会神经肿瘤专业委员会神经肿瘤研究项目(项目编号:CSNO-2014-MSD01)

作者单位:300052 天津医科大学总医院神经外科(杨亦寒、马海文、白宇、明浩朗、于圣平、任炳成、林雨、张凯、海龙、王伟、程铖、李涛、杨学军),PET-CT影像诊断科(蔡莉、王颖)

通讯作者:杨学军(Email:ydenny@yahoo.com)

grade Ⅲ; the peripheral edema of 7 cases (7/17) were grade Ⅰ and 10 cases (10/17) grade Ⅱ. The differences between TDL and glioma were statistically significant (Fisher's exact probability: P = 0.032, 0.024). ^{18}F-FDG PET and ^{11}C-MET PET were not statistically significant in differentiating TDL and glioma (Fisher's exact probability: P = 0.182, 0.081). **Conclusions** Mass effect and peripheral edema showed in MRI can be used for the differential diagnosis of TDL and glioma. The value of PET-CT in differentiating TDL and glioma is unsure.

【Key words】 Demyelinating diseases; Central nervous system; Glioma; Megnetic resonance imaging; Tomography, emission-computed

This study was supported by China Anti-Cancer Association Neuro-Oncology Research Project (No. CSNO-2014-MSD01).

颅内肿胀性脱髓鞘病变(TDL)是一种介于多发性硬化(MS)和急性播散性脑脊髓炎(ADEM)的中间形态,常发生于多发性硬化早期阶段[1],但从病理学方面区分二者仍有一定难度。颅内肿胀性脱髓鞘病变常在中枢神经系统形成小卵圆形病灶,病变具有同质性,与周围正常脑组织界限清晰。病灶≥2 cm是诊断颅内肿胀性脱髓鞘病变的标准[2]。不同于其他类型脱髓鞘病变,颅内肿胀性脱髓鞘病变仅存在单一病灶,除具有脱髓鞘病变普遍特点外,其临床症状还与病变部位有关[3],表现为局灶性神经功能缺损、癫痫发作、失语症等。明确诊断主要依靠临床表现,神经电生理学监测和脑脊液检查也可以提供有价值信息[4]。由于颅内肿胀性脱髓鞘病变在影像学上与颅内肿瘤相似,如CT表现为低于周围脑组织的较低密度影,增强MRI呈现不完整环状强化征象,因此,影像学检查对二者的鉴别诊断有重要意义。

尽管颅内肿胀性脱髓鞘病变具有一些鉴别诊断意义的特点,但在临床实践中与颅内肿瘤明确区分仍有困难,尤其是高级别胶质瘤[5]。明确诊断肿胀性脱髓鞘病变仍依靠病变组织活检术或试验性激素治疗,若症状有所缓解、影像学显示病变缩小,方可明确诊断[1]。

多模态影像学综合诊断理念的提出和多种影像学技术的临床应用,为中枢神经系统疾病的诊断与鉴别诊断带来更多极具价值的信息,一定程度上可以实现疾病早期诊断。尽管对于神经外科医师而言,外科手术仍是主要治疗方法,但是如果一些可以采取内科保守治疗的疾病在术前即明确诊断并予以有效治疗,避免手术创伤,亦极具临床意义。CT和MRI业已成为中枢神经系统脱髓鞘疾病和肿瘤的常规检测技术[6];PET-CT可以从代谢角度对疾病进行分析,对于难以早期诊断的颅内肿胀性脱髓鞘病变是否具有明确的诊断价值尚缺乏共识性意见。目前尚无MRI联合PET-CT鉴别诊断颅内肿胀性脱髓鞘病变与胶质瘤的报道。本研究采用MRI联合^{18}F-脱氧葡萄糖(^{18}F-FDG)PET和^{11}C-蛋氨酸(^{11}C-MET)PET显像对31例颅内肿胀性脱髓鞘病变与胶质瘤进行鉴别诊断,以期有助于提高颅内肿胀性脱髓鞘病变的早期诊断率及其与胶质瘤的鉴别诊断率,为临床诊断与治疗疾病提供依据。

资料与方法

一、临床资料

1. 纳入标准 (1)颅内肿胀性脱髓鞘病变的病灶≥2 cm,且部分经病理学证实、部分经内科保守治疗好转间接证实。(2)经病理学证实的胶质瘤。(3)均行头部MRI检查,若MRI明确诊断困难则进一步行^{18}F-FDG PET和^{11}C-MET PET显像。(4)本研究经天津医科大学总医院道德伦理委员会审批,所有患者或其家属均知情同意并签署知情同意书。

2. 排除标准 (1)经头部MRI或PET-CT能够明确诊断的颅内肿胀性脱髓鞘病变。(2)经头部MRI或PET-CT能够明确诊断的胶质瘤。(3)住院期间未能明确诊断。

3. 一般资料 选择2010年5月-2016年12月在天津医科大学总医院住院治疗并最终诊断为颅内肿胀性脱髓鞘病变或胶质瘤患者共31例,其中颅内肿胀性脱髓鞘病变14例,胶质瘤17例;男性11例,女性20例;年龄21~71岁,平均(49±12)岁。(1)颅内肿胀性脱髓鞘病变:共14例患者,男性2例,女性12例;年龄40~62岁,平均(49±8)岁;临床表现为头痛,呕吐,肢体和口角抽搐等癫痫样症状,言语不清和肢体活动不利等神经功能缺损症状。(2)胶质瘤:17例患者,男性9例,女性8例;年龄21~71岁,平均(49±14)岁;临床表现为头痛、头晕,恶心、呕

吐，肢体抽搐等癫痫样症状，言语障碍和肢体活动障碍等神经功能缺损症状。

二、研究方法

1. 头部MRI检查　采用德国Siemens公司生产的3.0T MRI扫描仪，20通道头部表面线圈，梯度场强80 mT/m，扫描序列包括T_1WI、T_2WI、FLAIR成像和扩散加权成像（DWI）。（1）T_1WI：重复时间（TR）2000 ms、回波时间（TE）7.40 ms，扫描视野（FOV）为24 cm×24 cm，矩阵320×320，激励次数（NEX）1次，层厚5 mm、层间距为零，共18层，扫描时间70 s，扫描范围覆盖颅底至颅顶全部脑组织。（2）T_2WI：重复时间4000 ms、回波时间88 ms，扫描视野为24 cm×24 cm，矩阵512×512，激励次数1次，层厚5 mm、层间距为零，共18层，扫描时间64 s，扫描范围覆盖颅底至颅顶全部脑组织。（3）FLAIR成像：重复时间4000 ms、回波时间88 ms，扫描视野24 cm×24 cm，矩阵512×512，激励次数1次，层厚5 mm、层间距为零，共18层，扫描时间64 s，扫描范围覆盖颅底至颅顶全部脑组织。（4）DWI序列：重复时间3100 ms、回波时间59和102 ms、反转时间（TI）1500 ms，扫描视野22 cm×22 cm，矩阵224×224，激励次数1次，层厚5 mm、层间距为零，共扫描18层，扫描时间85 s，扫描范围覆盖颅底至颅顶全部脑组织。MRI观察指标为：（1）病变与周围正常脑组织界限是否清晰。（2）T_1WI、T_2WI和DWI序列信号强度。（3）强化征象，包括环状强化和开环状强化等。（4）占位效应，0级，无占位效应；Ⅰ级，局部脑沟、脑池受压，脑室无受压变形，中线结构无移位；Ⅱ级，脑室受压变形，中线结构无移位；Ⅲ级，脑室受压变形，中线结构移位≤1 cm；Ⅳ级，中线结构移位>1 cm。（5）周围脑水肿，Ⅰ度，周围脑水肿宽度≤2 cm；Ⅱ度，周围脑水肿宽度>2 cm，但未超过同侧大脑半球1/2；Ⅲ度，周围脑水肿范围超出同侧大脑半球1/2。（6）是否存在病变中心静脉扩张。（7）是否累及胼胝体。（8）是否存在病变中心坏死。（9）是否累及灰质。

2. PET-CT显像　采用美国GE公司生产的Discovery PET/CT 710扫描仪，^{18}F-FDG和^{11}C-MET显像剂由天津医科大学总医院PET-CT影像诊断科自行合成，放射化学纯度和标记率>95%。所有患者禁食6 h以上，于安静、避光环境静脉注射^{18}F-FDG 222 MBq或^{11}C-MET 740 MBq，^{18}F-FDG静脉注射后50～60 min采集三维图像8 min、^{11}C-MET静脉注射后20 min采集三维图像8 min，PET-CT数据处理采用有序子集最大似然法（OSEM），获得横断面、冠状位和矢状位图像。对显像剂代谢程度进行视觉分析并将病变代谢程度分为3种类型：（1）低代谢，病变显像剂摄取程度低于或等于白质。（2）中度代谢，病变摄取程度高于白质但明显低于皮质。（3）高代谢，病变摄取程度接近于、等于或高于白质。

三、统计分析方法

采用SPSS 22.0统计软件进行数据处理与分析。计数资料以相对数构成比（%）或率（%）表示，采用Fisher确切概率法；呈正态分布的计量资料以均数±标准差（$\bar{x}\pm s$）表示。以$P\leq 0.05$为差异具有统计学意义。

结　果

一、MRI鉴别颅内肿胀性脱髓鞘病变与胶质瘤

MRI显示，颅内肿胀性脱髓鞘病变患者占位效应0级8例（8/14）、Ⅰ级4例（4/14）、Ⅱ级1例（1/14）、Ⅲ级1例（1/14），胶质瘤患者占位效应0级2例（2/17）、Ⅰ级6例（6/17）、Ⅱ级7例（7/17）、Ⅲ级2例（2/17），组间差异有统计学意义（Fisher确切概率法：$P=0.032$）；颅内肿胀性脱髓鞘病变患者周围脑水肿Ⅰ度12例（12/14）、Ⅱ度2例（2/14），胶质瘤患者周围脑水肿Ⅰ度7例（7/17）、Ⅱ度10例（10/17），组间差异有统计学意义（Fisher确切概率法：$P=0.024$）；而病变与周围正常脑组织界限清晰，T_1WI、T_2WI和DWI序列信号强度，强化征象（环状强化和开环状强化等），病变中心静脉扩张，胼胝体受累，病变中心坏死，灰质受累组间差异无统计学意义（均$P>0.05$，表1）。

二、^{18}F-FDG PET和^{11}C-MET PET显像鉴别颅内肿胀性脱髓鞘病变与胶质瘤

^{18}F-FDG PET和^{11}C-MET PET显像显示，颅内肿胀性脱髓鞘病变与胶质瘤患者^{18}F-FDG和^{11}C-MET代谢程度差异均无统计学意义（Fisher确切概率法：$P=0.182$，0.081；表2）。

典型病例

例1　女性，64岁，因头晕3.50个月，于2011年5月20日入院。患者于3.50个月前无明显诱因突发间断性头晕，休息后缓解，无头痛，无恶心、呕吐，无饮水呛咳，无四肢抽搐、口吐白沫，无大小便失禁，上述症状反复发作。外院行头部MRI检查（2011年5月15日）显示，右侧脑桥臂高信号影，增强扫描病

表1 颅内肿胀性脱髓鞘病变患者与胶质瘤患者MRI的比较[例(%)]

Table 1. Comparison of MRI features between TDL and glioma [case (%)]

Item	TDL (N = 14)	Glioma (N = 17)	*P* value	Item	TDL (N = 14)	Glioma (N = 17)	*P* value
Border clarity	1 (1/14)	1 (1/17)	1.000	Open-ring enhancement	2 (2/14)	0 (0/17)	0.196
T_1WI			1.000	Mass effect			
Hypointensity	3 (3/14)	4 (4/17)		0	8 (8/14)	2 (2/17)	0.032
Isointensity	0 (0/14)	1 (1/17)		Ⅰ	4 (4/14)	6 (6/17)	
Hyperintensity	11 (11/14)	12 (12/17)		Ⅱ	1 (1/14)	7 (7/17)	
T_2WI			0.773	Ⅲ	1 (1/14)	2 (2/17)	
Hypointensity	1 (1/14)	0 (0/17)		Ⅳ	0 (0/14)	0 (0/17)	
Isointensity	1 (1/14)	2 (2/17)		Peripheral edema			0.024
Hyperintensity	12 (12/14)	15 (15/17)		Ⅰ	12 (12/14)	7 (7/17)	
DWI			0.153	Ⅱ	2 (2/14)	10 (10/17)	
Hypointensity	4 (4/14)	2 (2/17)		Ⅲ	0 (0/14)	0 (0/17)	
Isointensity	1 (1/14)	6 (6/17)		Central venectasia	3 (3/14)	3 (3/17)	1.000
Hyperintensity	9 (9/14)	9 (9/17)		Corpus callosum engagement	5 (5/14)	1 (1/17)	0.067
Enhancement	7 (7/14)	13 (13/17)	0.153	Central necrosis	3 (3/14)	5 (5/17)	0.698
Ring enhancement	5 (5/14)	3 (3/17)	0.412	Gray matter engagement	3 (3/14)	5 (5/17)	0.698

TDL, tumefactive demyelinating lesion, 肿胀性脱髓鞘病变; DWI, diffusion-weighted imaging, 扩散加权成像

表2 脑肿胀性脱髓鞘病变与胶质瘤患者^{18}F-FDG PET和^{11}C-MET PET代谢程度的比较[例(%)]

Table 2. Comparison of PET-CT features between TDL and glioma [case (%)]

Item	TDL (N = 14)	Glioma (N = 17)	*P* value	Item	TDL (N = 14)	Glioma (N = 17)	*P* value
^{18}F-FDG PET			0.182	^{11}C-MET PET			0.081
Low intensity	6 (6/14)	4 (4/17)		Low intensity	2 (2/14)	0 (0/17)	
Isointensity	1 (1/14)	0 (0/17)		Isointensity	1 (1/14)	0 (0/17)	
High intensity	7 (7/14)	13 (13/17)		High intensity	11 (11/14)	17 (17/17)	

TDL, tumefactive demyelinating lesion, 肿胀性脱髓鞘病变; ^{18}F-FDG, ^{18}F-fluoro-2-deoxy-D-glucose, ^{18}F-脱氧葡萄糖; ^{11}C-MET, ^{11}C-methionine, ^{11}C-蛋氨酸

灶呈环状强化(图1a~1c),考虑颅内占位性病变。为求进一步诊断与治疗,遂至我院就诊。患者自发病以来,精神可,睡眠、饮食正常,大小便正常,体重无明显变化。既往史、个人史及家族史均无特殊。入院后体格检查:神志清楚,语言流利,对答切题;双侧瞳孔等大、等圆,直径约为3 mm,对光反应灵敏,眼球各向活动充分,双侧视野粗测正常,无眼震、复视,无双睑下垂;鼻唇沟对称,伸舌居中,口角无歪斜,颈部柔软;双侧肢体肌力5级,肌张力正常;生理反射存在,病理征阴性。^{11}C-MET PET显示,MRI所示病变同一位置蛋氨酸呈高代谢(图1d)。尽管^{11}C-MET PET呈现高代谢,但MRI所示占位效应并不明显,与占位大小不成正比。临床考虑为脱髓鞘病变。患者拒绝进一步治疗,共住院10 d后出院,1个月后随访,复查MRI,增强扫描显示原脑桥臂病灶呈开环状强化(图1e),最终明确诊断为肿胀性脱髓鞘病变。

例2 女性,62岁,主因右侧眼周肌肉抽搐并进行性加重1年,于2012年3月21日入院。患者1年前无明显诱因出现发作性右侧眼周肌肉抽搐,可自行缓解,无明显认知功能障碍,无头痛、头晕,无恶心、呕吐,无四肢抽搐、口吐白沫,无大小便失禁,症状进行性加重。外院行头部MRI检查(2012年3月15日)显示,双侧额颞枕叶、双侧岛叶、左侧放射冠和胼胝体广泛高信号影,中线结构受压向右侧偏移(图2a),考虑多发性脱髓鞘病变,不排除胶质瘤。为求进一步诊断与治疗,遂至我院就诊。患者自发病以来,精神可,睡眠、饮食正常,大小便正常,体重无明显变化。既往史、个人史及家族史均无特殊。入院后体格检查:神志清楚,语言流利,对答切题;双侧瞳孔等大、等圆,直径约为3 mm,对光反应灵敏,眼球各向活动充分,双侧视野粗测正常,无眼

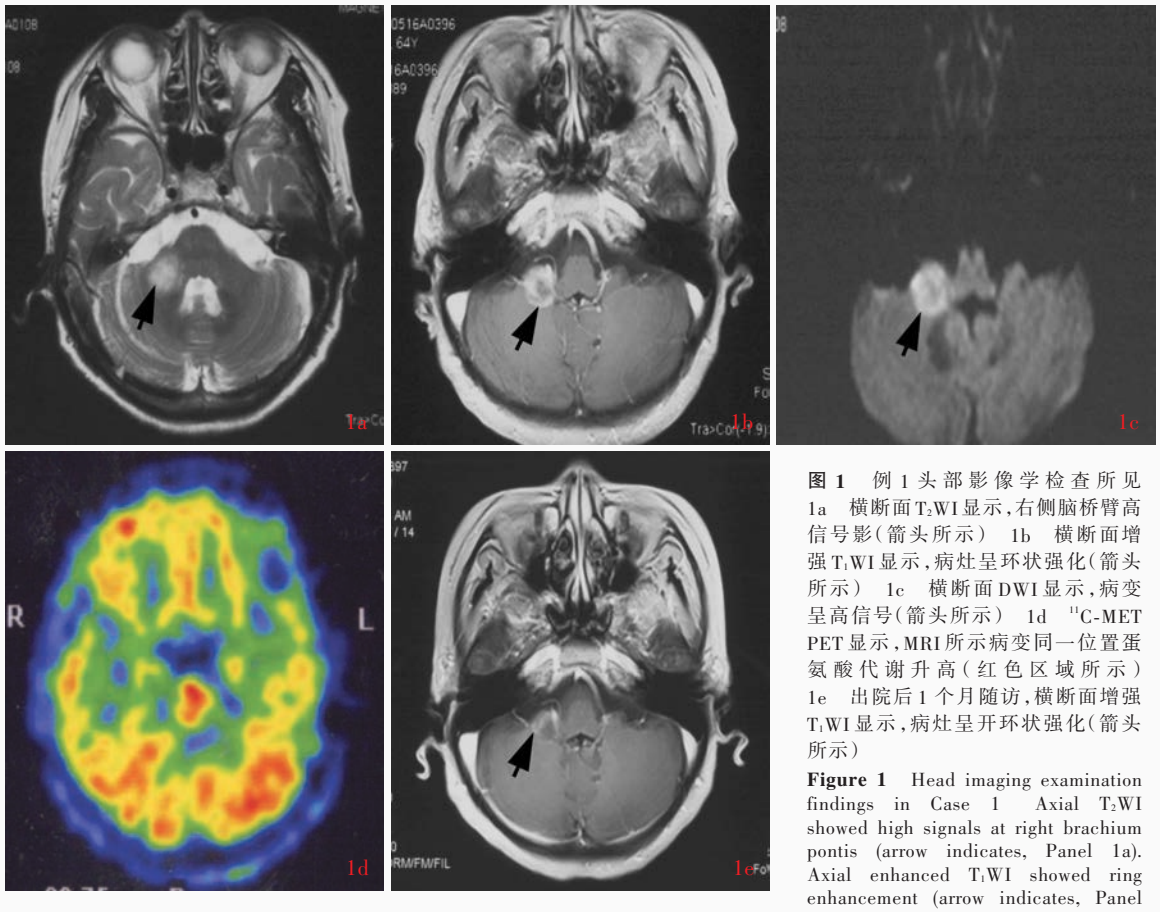

图1 例1头部影像学检查所见 1a 横断面T_2WI显示，右侧脑桥臂高信号影（箭头所示） 1b 横断面增强T_1WI显示，病灶呈环状强化（箭头所示） 1c 横断面DWI显示，病变呈高信号（箭头所示） 1d ^{11}C-MET PET显示，MRI所示病变同一位置蛋氨酸代谢升高（红色区域所示） 1e 出院后1个月随访，横断面增强T_1WI显示，病灶呈开环状强化（箭头所示）

Figure 1 Head imaging examination findings in Case 1 Axial T_2WI showed high signals at right brachium pontis (arrow indicates, Panel 1a). Axial enhanced T_1WI showed ring enhancement (arrow indicates, Panel 1b). Axial DWI showed a high signals lesion (arrow indicates, Panel 1c). ^{11}C-MET PET showed ^{11}C-MET metabolic elevation at the same lesion shown in MRI (red areas indicate, Panel 1d). One month after discharge, axial enhanced T_1WI showed open-ring enhancement (arrow indicates, Panel 1e).

震、复视，无双睑下垂；鼻唇沟对称，伸舌居中，口角无歪斜，颈部柔软；双侧肢体肌力5级，肌张力正常；生理反射存在，病理征阴性。^{18}F-FDG PET显示，MRI所示病变同一位置无葡萄糖异常聚集（图2b）；^{11}C-MET PET显示，MRI所示病变同一位置无蛋氨酸异常聚集（图2c），提示非典型肿瘤征象。临床诊断为脱髓鞘病变，转入神经内科行激素序贯疗法，即甲泼尼龙500 mg/d加入生理盐水250 ml中静脉滴注3 d，再甲泼尼龙240 mg/d加入生理盐水100 ml中静脉滴注3 d，再甲泼尼龙120 mg/d加入生理盐水100 ml中静脉滴注3 d，再甲泼尼龙80 mg/d加入生理盐水100 ml中静脉滴注3 d，再甲泼尼龙40 mg/d加入生理盐水100 ml中静脉滴注3 d，临床症状略有减轻。患者共住院32 d，出院后6个月随访，复查MRI显示病变高信号减轻（图2d）；复查^{18}F-FDG PET和^{11}C-MET PET未见放射性元素异常聚集（图2e，2f）。最终证实为肿胀性脱髓鞘病变。

讨　论

颅内肿胀性脱髓鞘病变的诊断“金标准”是病变组织活检术，缺乏其他较准确的诊断标准。

一、MRI鉴别颅内肿胀性脱髓鞘病变与胶质瘤

MRI检查对颅内肿胀性脱髓鞘病变的诊断有一定价值[7]。该病好发于脑白质，且常为邻近脑室的白质[8]。早期临床症状不具有特异性，T_1WI呈低信号[9]，增强扫描病灶可能无明显对比增强[8,10]，也可能出现环状或开环状强化[8,10-12]。MRI检查常提示与病灶大小不符的占位效应和周围脑水肿[8-9,11,13]。MRI随访可见更典型的肿胀性脱髓鞘病变特征，如开环状强化逐渐显现，此外，还可见病变中心静脉扩张[11]。

然而，单一MRI检查对鉴别诊断颅内肿胀性脱髓鞘病变与胶质瘤具有局限性。本研究行单一MRI检查即不足以证实病变为肿胀性脱髓鞘病变或胶

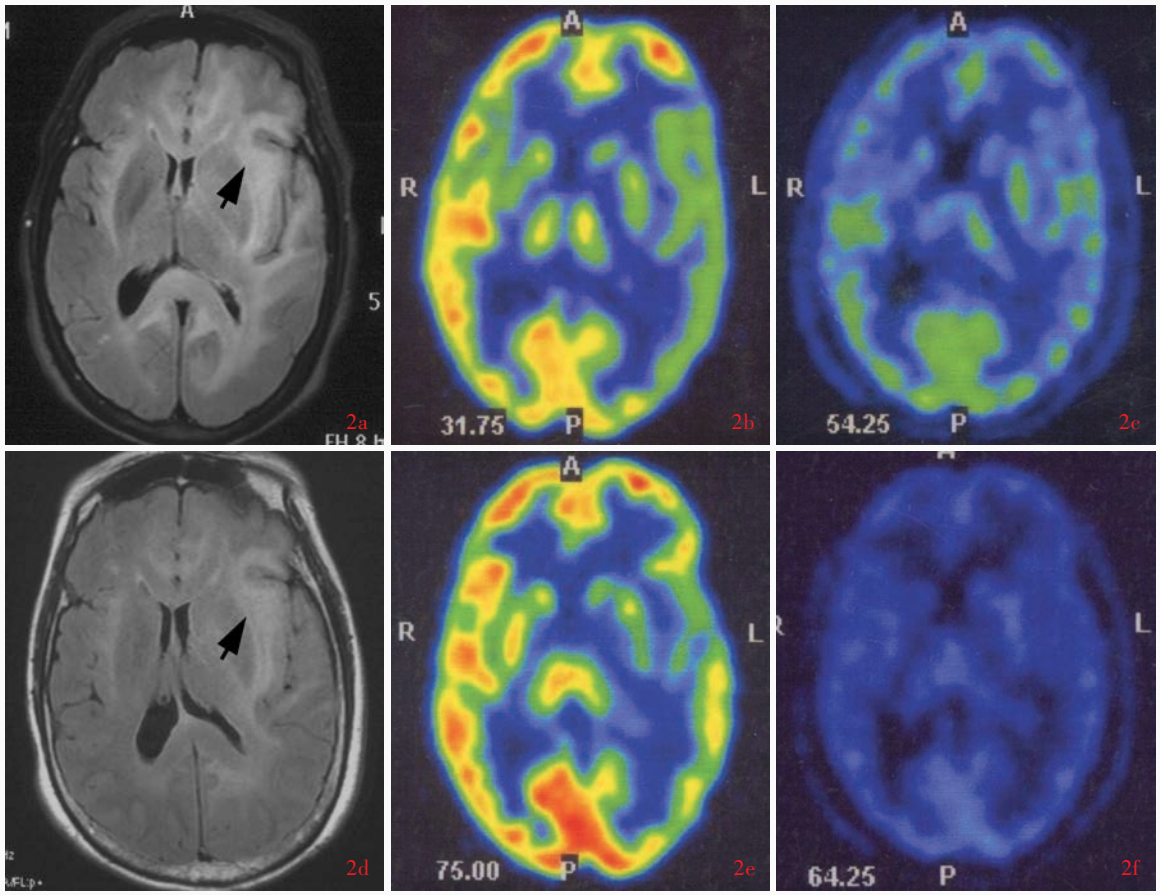

图2 例2头部影像学检查所见 2a 横断面FLAIR成像显示，深部白质弥漫性高信号影（箭头所示） 2b ^{18}F-FDG PET显示，MRI所示病变同一位置无葡萄糖异常聚集 2c ^{11}C-MET PET显示，MRI所示病变同一位置无蛋氨酸异常聚集 2d 出院后6个月随访，横断面FLAIR成像显示，病变高信号减轻（箭头所示） 2e ^{18}F-FDG PET未见葡萄糖异常聚集 2f ^{11}C-MET PET未见蛋氨酸异常聚集

Figure 2 Head imaging examination findings in Case 2 Axial FLAIR showed diffusing high signals in deep white matter (arrow indicates, Panel 2a). ^{18}F-FDG PET showed no abnormal concentration of ^{18}F-FDG at the same lesion shown in MRI (Panel 2b). ^{11}C-MET PET showed no abnormal concentration of ^{11}C-MET at the same lesion shown in MRI (Panel 2c). Six months after dischange, axial FLAIR showed the high signals attenuated (arrow indicates, Panel 2d). Six months after discharge, ^{18}F-FDG PET showed no abnormal concentration of ^{18}F-FDG (Panel 2e). Six months after discharge, ^{11}C-MET PET showed on abnormal concentration of ^{11}C-MET (Panel 2f).

质瘤。肿胀性脱髓鞘病变不一定呈现出上述MRI特征[14]，炎症急性期可以表现出与某些低级别胶质瘤相似的影像学特征[8-9]，如某些肿胀性脱髓鞘病变MRI可见病变沿胼胝体进展，与胶质瘤类似[8,13]，亦可见与胶质瘤相似的灰质受累[11]。此外，肿胀性脱髓鞘病变可能存在不够清晰和规整的边界[11]。占位效应明显的肿胀性脱髓鞘病变易误诊为肿瘤[8]，亦有胶质瘤呈现开环状强化征象[15]。

在本研究中，采用MRI鉴别诊断颅内肿胀性脱髓鞘病变与胶质瘤时，占位效应和周围脑水肿差异有统计学意义，与临床实践经验相符：肿胀性脱髓鞘病变作为炎症性疾病，占位效应不甚明显，且病变周围水肿带也不如胶质瘤明显。其他MRI指标两种疾病比较差异无统计学意义，究其原因，这些MRI特点对两种疾病的鉴别诊断可能不具有明确的价值，如肿胀性脱髓鞘病变急性期，确实会出现强化征象，给鉴别诊断带来困难，但本研究为回顾性研究，样本量较小，采用小样本统计学方法，有些MRI指标虽不具有统计学意义，但P值接近0.05，尚待基于相同目的的前瞻性研究、纳入更大样本量、采用大样本统计学方法，可能得到更接近真实的结果。尽管MRI显示的占位效应和周围脑水肿对鉴别诊断颅内肿胀性脱髓鞘病变与胶质瘤具有统计学意义，但是在临床实践中，对于难以确定的颅内占位性病变，仅凭MRI显示的占位效应和周围脑水肿进行诊断远远不够，还应进行PET-CT检查。

二、不同显像剂PET-CT鉴别颅内肿胀性脱髓鞘病变与胶质瘤

既往PET-CT用于鉴别诊断颅内肿胀性脱髓鞘病变与胶质瘤的价值不明确。颅内肿胀性脱髓鞘病变患者^{18}F-FDG PET亦可见与胶质瘤相似的葡萄糖高代谢[16]。但有文献报道,^{18}F-FDG PET显示葡萄糖低代谢更具鉴别诊断价值[17]。仅少量病例报道证实PET-CT显像对鉴别诊断颅内肿胀性脱髓鞘病变与胶质瘤有益[18]。某些具有胶质瘤MRI特征的肿胀性脱髓鞘病变PET-CT显像并未显示出明显的高代谢,而仅表现为中度摄取[6]或仅围绕病灶的环状高代谢区域[19],这些PET-CT指标对于鉴别诊断颅内肿胀性脱髓鞘病变与胶质瘤是否有临床意义,尚未见诸报道。

本研究结果显示,^{18}F-FDG PET和^{11}C-MET PET显像对颅内肿胀性脱髓鞘病变与胶质瘤的鉴别诊断无明确作用,究其原因,可能有以下两点:首先,肿胀性脱髓鞘病变急性期PET-CT可能呈现出与胶质瘤相似的高代谢。本研究纳入的患者大部分处于炎症急性期,就显像剂代谢而言,出现类似胶质瘤的高代谢是合理的。此种情况下,反观MRI征象,高度怀疑为肿胀性脱髓鞘病变。其次,本研究样本量较小,尚待大样本临床试验进一步研究。此外,在本研究中,^{18}F-FDG和^{11}C-MET并未显示出明显不同和优缺点,亦待大样本临床研究加以区分。

总之,临床鉴别诊断颅内肿胀性脱髓鞘病变与胶质瘤有一定困难,尤以肿胀性脱髓鞘病变早期或急性期,鉴别诊断难度最大[20],有可能出现MRI联合PET-CT无法鉴别诊断的情况,对于此类患者,疑似颅内肿胀性脱髓鞘病变时可采用其他特异性检测方法,如腰椎穿刺脑脊液检查,测定寡克隆区带(OB)等特征性指标,如果上述特异性指标呈阳性,则更倾向于颅内肿胀性脱髓鞘病变;若未经治疗,复查MRI可见逐渐呈现的开环状强化,则高度提示颅内肿胀性脱髓鞘病变;此外,^{23}Na MRI也可能为颅内肿胀性脱髓鞘病变的提供诊断信息[21]。

综上所述,本研究结果显示,基于MRI特征鉴别诊断颅内肿胀性脱髓鞘病变与胶质瘤科学、可靠,但仍有MRI表现不甚典型的颅内肿胀性脱髓鞘病变,此时有条件的医疗中心可进一步行^{18}F-FDG PET和^{11}C-MET PET显像,从而提供更加准确的诊断信息,当难以鉴别的病灶呈现低代谢时,高度提示颅内肿胀性脱髓鞘病变的可能。

参 考 文 献

[1] Dagher AP, Smirniotopoulos J. Tumefactive demyelinating lesions. Neuroradiology, 1996, 38:560-565.

[2] Lucchinetti CF, Gavrilova RH, Metz I, Parisi JE, Scheithauer BW, Weigand S, Thomsen K, Mandrekar J, Altintas A, Erickson BJ, König F, Giannini C, Lassmann H, Linbo L, Pittock SJ, Brück W. Clinical and radiographic spectrum of pathologically confirmed tumefactive multiple sclerosis. Brain, 2008, 131:1759-1775.

[3] Algahtani H, Shirah B, Alassiri A. Tumefactive demyelinating lesions: a comprehensive review. Mult Scler Relat Disord, 2017, 14:72-79.

[4] Polman CH, Reingold SC, Banwell B, Clanet M, Cohen JA, Filippi M, Fujihara K, Havrdova E, Hutchinson M, Kappos L, Lublin FD, Montalban X, O'Connor P, Sandber-Wollheim M, Thompson AJ, Waubant E, Weinshenker B, Wolinsky JS. Diagnostic criteria for multiple sclerosis: 2010 revisions to the McDonald criteria. Ann Neurol, 2011, 69:292-302.

[5] Mabray MC, Cohen BA, Villanueva-Meyer JE, Valles FE, Barajas RF, Rubenstein JL, Cha S. Performance of apparent diffusion coefficient values and conventional MRI features in differentiating tumefactive demyelinating lesions from primary brain neoplasms. AJR Am J Roentgenol, 2015, 205:1075-1085.

[6] He GN, Han X, Wang EF, Wang LM, Yuan LP, Li YW, Yan X. Differential diagnosis of cervical spinal cord demyelinating diseases and cervical intramedullary gliomas. Zhongguo Xian Dai Shen Jing Ji Bing Za Zhi, 2014, 14:789-794.[贺桂女, 韩雄, 王恩锋, 王莉梅, 袁丽品, 李艳伟, 晏僖. 颈髓脱髓鞘病变与髓内胶质瘤的鉴别诊断. 中国现代神经疾病杂志, 2014, 14:789-794.]

[7] Preziosa P, Martinelli V, Moiola L, Radaelli M, Gerevini S, Guidetti D, Immovilli P, Michieletti E, Scagnelli P, Comola M, Rocca MA, Filippi M, Comi G. Dynamic pattern of clinical and MRI findings in a tumefactive demyelinating lesion: a case report. J Neurol Sci, 2016, 361:184-186.

[8] Friedman DI. Multiple sclerosis simulationg a mass lesion. J Neuroophthalmol, 2000, 20:147-153.

[9] Kim DS, Na DG, Kim KH, Kim JH, Kim E, Yun BL, Chang KH. Distinguishing tumefactive demyelinating lesions from glioma or central nervous system lymphoma: added value of unenhanced CT compared with conventional contrast-enhanced MR imaging. Radiology, 2009, 251:467-475.

[10] Ninomiya S, Hara M, Morita A, Teramoto H, Momose M, Takahashi T, Kamei S. Tumefactive demyelinating lesion differentiated from a brain tumor using a combination of magnetic resonance imaging and (11)C-methionine positron emission tomography. Intern Med, 2015, 54:1411-1414.

[11] Given CA 2nd, Stevens BS, Lee C. The MRI appearance of tumefactive demyelinating lesions. AJR Am J Roentgenol, 2004, 182:195-199.

[12] Siri A, Carra-Dalliere C, Ayrignac X, Pelletier J, Audoin B, Pittion-Vouyovitch S, Debouverie M, Lionnet C, Viala F, Sablot D, Brassat D, Ouallet JC, Ruet A, Brochet B, Taillandier L, Bauchet L, Derache N, Defer G, Cabre P, de Seze J, Lebrun Frenay C, Cohen M, Labauge P. Isolated tumefactive demyelinating lesions: diagnosis and long-term evolution of 16 patients in a multicentric study. J Neurol, 2015, 262:1637-1645.

[13] Kurihara N, Takahashi S, Furuta A, Higano S, Matsumoto K, Tobita M, Konno H, Sakamoto K. MR imaging of multiple sclerosis simulating brain tumor. Clin Imaging, 1996, 20:171-177.

[14] Villa A, Quarracino C, Colobraro A. Pseudotumoral lesion:

pathology and follow-up. Acta Neurol Belg, 2016, 116:627-628.
[15] Kinon MD, Scoco A, Farinhas JM, Kobets A, Weidenheim KM, Yassari R, Lasala PA, Graber J. Glioblastoma multiforme presenting with an open ring pattern of enhancement on MR imaging. Surg Neurol Int, 2017, 8:106.
[16] Schiepers C, Van Hecke P, Vandenberghe R, Van Oostende S, Dupont P, Demaerel P, Bormans G, Carton H. Positron emission tomography, magnetic resonance imaging and proton NMR spectroscopy of white matter in multiple sclerosis. Mult Scler, 1997, 3:8-17.
[17] Bakshi R, Miletich RS, Kinkel PR, Emmet ML, Kinkel WR. High - resolution fluorodeoxyglucose positron emission tomography shows both global and regional cerebral hypometabolism in multiple sclerosis. J Neuroimaging, 1998, 8: 228-234.
[18] Chiavazza C, Cistaro A, Fania P, Bertolotto A, Cavalla P, Rudà R, Pinessi L, Soffietti R. Reversible disconnection syndrome in a case of acute tumefactive demyelinating lesion: a PET study. Neurol Sci, 2016, 37:2019-2023.
[19] Dong A, Gao M, Wang Y, Gao L, Zuo C. FDG PET/CT in acute tumefactive multiple sclerosis occurring in a case of chronic graft - versus - host disease after allogeneic hematopoietic stem cell transplantation. Clin Nucl Med, 2016, 41:E414-416.
[20] Conforti R, Capasso R, Galasso R, Cirillo M, Taglialatela G, Galasso L. A challenging diagnosis of late - onset tumefactive multiple sclerosis associated to cervicodorsal syringomyelia: doubtful CT, MRI, and bioptic findings: case report and literature review. Medicine (Baltimore), 2016, 95:E4585.
[21] Huhn K, Mennecke A, Linz P, Tschunko F, Kästle N, Nagel AM, Uder M, Dörfler A, Linker RA, Engelhorn T. 23Na MRI reveals persistent sodium accumulation in tumefactive MS lesions. J Neurol Sci, 2017, 379:163-166.

（收稿日期：2017-09-02）

Epigenetic Methods in Neuroscience Research published

Epigenetic Methods in Neuroscience Research (ISBN: 978-1-4939-2753-1, eBook ISBN: 978-1-4939-2754-8) was published by Springer in 2016. The editor of this book is Nina N. Karpova, Neuroscience Center, University of Helsinki.

This volume presents state-of-the-art methods for reliable detection of epigenetic changes in the nervous system. *Epigenetic Methods in Neuroscience Research* guides readers through methods for the analyses of chromatin remodeling, transposable elements, non-coding RNAs, such as micro RNAs (miRNAs), and circadian oscillations, including: analysis of DNA methylation in neuronal and glial cells or small tissue samples; sensitive method for quantification of alternative methylated forms of cytosines by liquid chromatography/mass spectrometry; affinity-based detection of modified cytosines by immunohistochemistry or methylated DNA immunoprecipitation; chromatin immunoprecipitation (ChIP); miRNA high-throughput profiling and the in situ detection of miRNA subtle expression in the brain; analysis of genes with alternative 3′ untranslated regions (3′UTRs); and the cite-specific delivery of chromatin-modifying drugs. Written in the popular Neuromethods series style, chapters include the kind of detail and key advice from the specialists needed to get successful results in your own laboratory.

Concise and easy-to-use, *Epigenetic Methods in Neuroscience Research* provides multidisciplinary epigenetic approach to study genome, and neural, plasticity that will help the reader to successfully address the challenges associated with neurodevelopmental, psychiatric, and neurodegenerative disorders.

The price of eBook is 79.72€, and hardcover is 94.99€. Visit link.springer.com for more information.

Epilepsy Towards the Next Decade published

Epilepsy Towards the Next Decade (ISBN: 978-3-319-12282-3, eBook ISBN: 978-3-319-12283-0) was published by Springer International Publishing in 2015. The editor of this book is Pasquale Striano, Pediatric Neurology and Muscular Diseases Unit, University of Genoa.

This volume is a comprehensive collection of the most recent knowledge on the biological bases of various kinds of epilepsies and modern clinical approaches to their treatment. Epilepsy affects about 0.5%-1.0% of the world′s population and the main goal of its treatment is to eliminate seizures without creating side effects. Despite numerous advances in the treatment of epilepsy and the approval of several new antiepileptic drugs, about 30% of patients continue to experience recurrent seizures which are medically, physically, and/or socially disabling. The editor of this volume hopes that by bridging the gap between the fundamental biology of epilepsy and its clinical implications he might spur further research and treatment options.

The price of eBook is 118.99€, and hardcover is 139.99€. Visit link.springer.com for more information.